Electronic structure of quasicrystalline Al-Zn-Mg alloys and related crystalline, amorphous, and liquid phases

J. Hafner and M. Krajčí*

Institut für Theoretische Physik, Technische Universität Wien, Wiedner Hauptstrasse 8-10, A-1040 Wien, Austria

(Received 9 November 1992)

We have studied the electronic structure of higher-order rational approximants to the icosahedral Al-Zn-Mg quasicrystal and of related crystalline, liquid, and amorphous phases. For the crystalline phases, self-consistent calculations using the linear muffin-tin orbital (LMTO) method have been performed, and the electronic structure of the higher-order approximants (with up to 12 380 atoms in the periodically repeated cell) and of the amorphous and liquid alloys has been calculated using the recursion method and a tight-binding LMTO method. Structure-induced pseudogaps at the Fermi level are predicted for the stable Frank-Kasper phase and for the higher-order approximants to the quasicrystal, but also for the amorphous alloy and some crystalline compounds. Hence, we conclude that although the pseudogap is a *generic* property of the quasicrystal, it is not a *specific* property distinguishing the quasiperiodic from the periodic or aperiodic phases. Crystalline, quasicrystalline, and amorphous alloys have to be considered as Hume-Rothery phases with a varying degree of band-gap stabilization.

I. INTRODUCTION

The discovery of quasicrystals,[1] i.e., of structures that possess perfect orientational, but only quasiperiodic translational long-range order, has raised many interesting questions. Are the electronic states in quasicrystals extended (like in crystals) or localized (like in amorphous materials)? The lack of translational periodicity means that Bloch's theorem is not applicable and that localized states may exist. On the other hand, one of the characteristic properties of quasicrystals besides their quasiperiodicity is the existence of a uniform distribution of local environments. For example, the Penrose lattice is quasiperiodic and self-similar (Penrose local isomorphism), and this means that for any local arrangement of diameter d, there exists a duplicate within a distance $2d$ (Conway's theorem[2]). The consequence is that even if an exponentially localized wave packet exists within a region of a diameter d, it can transfer to a region with the same structure within a distance $2d$, assisted by the overlapping tails of the wave functions. Conway's theorem suggests the existence of propagating states. In essence, this scenario has been confirmed by investigations of the eigenstates of very simple model Hamiltonians on one- and two-dimensional quasilattices.[3–6] It was found that most eigenstates are critical, i.e., neither extended nor localized, and that the power-law decay of the eigenstates is caused by competition between nonperiodicity and self-similarity. However, it has been also shown[7,8] that propagating eigenstates (i.e., states with a well-defined wave vector) can exist in a vicinity of certain quasiperiodically distributed points in wave-number space[9] (the Γ points of the quasilattice) and that strictly localized eigenstates associated with certain highly degenerate eigenvalues may exist.[10]

A second open question is why nature should prefer quasiperiodic to periodic order. There is, of course, the possibility of entropic stabilization, but there is sufficient evidence that perfectly ordered quasicrystals exist[11] and there are also many indications that the stability of quasicrystals is intimately related to their electronic structure.[12–16] The stoichiometry of many quasicrystalline phases appears to be governed by a Hume-Rothery-type rule, placing the Fermi level into a minimum of the electronic density of states. Theoretical arguments in favor of an electronically driven Hume-Rothery mechanism for stabilizing quasicrystals are based on nearly-free-electron theory and on electronic structure calculations for the lowest-order crystalline approximants to the quasicrystalline phases. One should also remember that Hume-Rothery-type arguments have also been brought forward for the stability (or rather metastability) of glassy materials[17,18] so that the question arises as to the differences in the Hume-Rothery stabilization of crystalline, quasicrystalline, and amorphous phases.

The third major problem relating to the electronic properties of quasicrystals is the explanation of their unusual transport properties.[19] Stable quasicrystals have semimetallic transport properties characterized by a high resistivity, a negative temperature coefficient of the resistivity, and strong temperature and composition dependences of the Hall coeficient and the thermopower. The unusual electronic properties of the ordered quasicrystals have been attributed to icosahedral symmetry which provides a unique structure factor for the Fermi-surface Brillouin-zone interactions. On the other hand, the disordered quasicrystals possess more metallic-glass-like transport properties.

The purpose of our present paper is to present the results of systematic investigations of the electronic properties of icosahedral alloys of the Frank-Kasper (Al-Zn-Mg) type and related amorphous and liquid alloys. In one dimension, the calculation of the electronic spec-

trum may be based on the real-space renormalization transformation of the Hamiltonian, owing to the scaling transformation of the quasilattice.[3,4] In two dimensions the exact renormalization procedure is possible only for a few specific Hamiltonians.[20] The alternative is to use the "commensurate" approximation. A quasiperiodic lattice can be constructed by projecting a "strip" of a six-dimensional lattice onto a three-dimensional physical space. If we replace in the icosahedral basis of the space perpendicular to the physical space the golden mean $\tau = (1+\sqrt{5})/2$ by a rational approximation $\tau_n = F_{n+1}/F_n$ (where the F_n are Fibonacci numbers), $n = 0,1,2\ldots$, we obtain a hierarchy of periodic Penrose lattices, converging to the quasiperiodic structure. These periodic lattices are the rational approximants of the quasilattice. The length of their period increases with increasing order of the approximant.

The three-dimensional (3D) Penrose lattices form the basic framework (the quasi-Bravais lattice) for the icosahedral quasicrystals.[21–23] In a real quasicrystal, the quasiperiodically repeated units (the Penrose tiles) have to be decorated with atoms. The construction of the decoration is facilitated by the fact that in some cases a low-order approximant to the quasicrystal is a known crystalline phase. For example, the crystal structure[24] of the Frank-Kasper phase $(Al,Zn)_{49}Mg_{32}$ is the $n = 1$, $\tau_1 = 1/1$ approximant to the Al-Zn-Mg quasicrystal.[25]

In the commensurate approximation for the calculation of the electronic structure, the quasiperiodic lattice is replaced by the periodic lattices of the rational approximants. For the periodic lattices conventional band-structure methods may be used. The justification for using the commensurate approximation derives from the fact that not only the scattering intensities calculated for the higher-order approximants converge rapidly to that measured for the icosahedral phase,[8,26] but also the electronic transport properties converge quickly in the series of the approximants. A particularly striking example is provided by the icosahedral phases in the (Al_xGa_{1-x})-Zn-Mg system.[27] Quasicrystals are formed over the entire range $0 \le x \le 1$. The quasicrystal with $x = 0$ is thermodynamically stable upon heating almost to the melting point. Quasicrystals with $0.2 \le x \le 0.5$, $0.6 \le x \le 0.7$, and $0.7 \le x \le 1.0$ transform into the orthorhombic $(3/2-2/1-2/1)$ and the cubic $(2/1-2/1-2/1)$ and $(1/1-1/1-1/1)$ approximants, respectively.[27–29] It has been shown that the electric resistivity of the $(1/1-1/1-1/1)$ approximant is about 70% of that of the quasicrystal and that the resistivities of the $(2/1-2/1-2/1)$ and $(3/2-2/1-2/1)$ approximants are nearly equal to that of the quasicrystal. Even more important, electronic specific-heat measurements have shown that the electronic density of states at the Fermi level for the three approximants remains essentially unchanged compared to that of the corresponding quasicrystal.[30]

However, even for the rational approximants, the calculation of the electronic structure remains a formidable task. Using the most efficient computer codes [such as, for example, the linear muffin-tin orbital method in the atomic-sphere approximation[31] (LMTO-ASA)], the self-consistent electronic structure can be obtained only for the lowest-order approximants with typically ≤ 100 inequivalent sites (which are often identical with stable crystalline structures). Such calculations have been performed for α-AlMn,[33] R-AlCuLi, $Al_{13}Fe_4$,[34] and $(Al,Zn)_{49}Zn_{32}$;[16] all are (1/1) approximants to the corresponding quasicrystals. Hence the challenge is to extend the electronic structure calculations to the higher-order approximants.

In this paper we present calculations of the electronic structure of the (2/1), (3/2), and (5/3) approximants of the Al-ZnMg quasicrystals with 688, 2920, and 12 380 atomic sites in the periodically repeated cell. Our calculations are based on the tight-binding (TB) variant of the LMTO method[35,36] and the real-space recursion technique[37,38] for the calculation of projected densities of state. Our results show that the density-of-states (DOS) minimum at the Fermi energy exists not only for the Frank-Kasper phase, but is a generic property of all higher-order approximants and hence probably also of the quasicrystal. The calculation of the Bloch spectral functions (i.e., of the densities of states projected onto states with a fixed wave vector) allows us to elucidate the quasiperiodic dispersion relations for the electronic states and the mechanism for the formation of a pseudogap at the Fermi energy. We also find that the dispersion relations are nearly stationary close to the Fermi edge, leading to a very low Fermi velocity. The combination of both results—reduced density of states at E_F (and hence a reduced number of carriers) and reduced Fermi velocity—goes a long way towards an explanation of the unusual transport properties of quasicrystals.

In addition to the investigation of the quasicrystalline phase, we calculate the electronic properties of the corresponding liquid and amorphous phases. We find that even in the complete absence of translational periodicity, the existence of a sharp first diffraction peak in the static structure factor leads to a shallow structure-induced DOS minimum at the Fermi energy. However, the amorphous phase receives much less band-gap stabilization than the quasicrystalline phase. This explains its lower stability. Dispersion relations are well defined only in the long-wavelength limit; for larger momentum transfer, the energy–wave-vector relation is quickly randomized.

In Sec. II we review very briefly the construction of the structure models for the rational approximants and the molecular-dynamics simulations of the liquid and amorphous phases. Section III presents the technical details of the TB-LMTO calculations of the electronic structure. The results for the rational approximants and for the liquid and amorphous phases are presented in Sec. IV. The Hume-Rothery mechanism for the stability of the quasicrystal is discussed in Sec. VI, and we conclude in Sec. VII.

II. STRUCTURAL MODELING

A. Construction of quasilattice

The 3D Penrose lattice can be generated by the projection method.[39,40] The projection method is based on

projecting a "strip" of a six-dimensional (6D) hypercubic lattice L_6 onto the 3D physical space E_3. The strip is defined by extending a unit cube in L_6 parallel to E_3. The orientation of E_3 is defined in such a way that the projection of a star of orthogonal basis vectors in L_6 forms an icosahedral basis in E_3, $\mathbf{e}_l = C(0,1,\tau)$+cyclic permutations (c.p.), $l = 1,2,3$, and $\mathbf{e}_l = C(0,-1,\tau)$+c.p., $l = 4,5,6$, where τ is the golden mean and C is a constant normalizing the basis vectors to unity. The projection of the 6D unit cube onto a 3D space E_3' perpendicular to E_3 is a rhombic triacontahedron, the acceptance domain for vertices of the quasilattice. A vertex of L_6 belongs to the quasilattice only if its projection onto E_3' falls into the acceptance domain.

The lattice of the crystalline approximants is obtained if in the icosahedral basis in E_3', $\mathbf{e}'_l = C'(0,-\tau,-1)$+c.p., $l = 1,2,3$, and $\mathbf{e}'_l = C'(0,\tau,1)$+c.p., $l = 4,5,6$, the golden mean τ is replaced by a rational number $\tau_n = F_{n+1}/F_n$, where the F_n are Fibonacci numbers, $F_0 = 0$, $F_1 = 1$, and $F_{n+1} = F_n + F_{n-1}$. The icosahedral basis in E_3 is unchanged. The lattice created by this projection is a periodic Penrose lattice (PPL). It can be viewed as a tiling of two kinds of golden rhombohedra: prolate (PR) and oblate (OR) ones. The lattice has cubic symmetry. We denote the approximants by F_{n+1}/F_n, the pair of Fibonacci numbers corresponding to the approximation τ_n to the golden mean τ.

B. Decoration of quasilattice by atoms

For the icosahedral alloys of the Al-Zn-Mg class the Penrose tiling is decorated as proposed by Henley and Elser.[25] In addition to the PR's and OR's a rhombic dodecahedron (RD) consisting of two PR's and two OR's is proposed as a composite structural unit. In the Henley-Elser decoration Al(Zn) atoms occupy all vertices and the midpoints of all edges of the structural units. Two Mg atoms are placed along the trigonal axis in each PR, including the PR's inside the RD. A special decoration is proposed for the fourfold vertex inside a RD: Four Mg atoms are placed on the edges originating from the fourfold vertex. Altogether eight Mg atoms inside a RD form a slightly distorted hexagonal bipyramid. The distribution of the Al and Zn sites over possible lattice sites is assumed to be random. We constructed the following structural models of Al-Zn-Mg quasicrystalline approximants: 1/1, 2/1, 3/2, and 5/3 with 162, 688, 2920, and 12 380 atoms in the unit cell, respectively. For more details we refer the reader to Ref. 26.

C. Molecular-dynamics annealing of idealized structural models

We relaxed our idealized quasicrystalline structures using a molecular-dynamics (MD) annealing at room temperature. Interatomic forces were calculated using pseudopotential perturbation theory. We used the optimized orthogonal-plane-wave-based pseudopotential[41,42] and the Ichimaru-Utsumi[43] local-field corrections to the dielectric function. For simplicity the ternary alloy (Al,Zn)Mg is treated as a quasibinary system (details are given in Ref. 26).

The MD simulations were performed for the 1/1 to 5/3 approximants, i.e., for ensembles with N=162 to N=12 380 particles in a periodically repeated cubic box. The simulations were performed in the microcanonical ensemble; temperature was controlled by a scaling of the velocities. The Newtonian equations of motions have been integrated using a fourth-order predictor-corrector algorithm in the Nordsieck formulation,[44] with a time increment of $\Delta t = 0.5 \times 10^{-15}$ s. For the lowest-order approximant, the potential was truncated at the largest distance compatible with the minimum image convention, $R_{\rm cut} \approx 7.00$ Å. For the larger models, the cutoff was extended to $R_{\rm cut} \approx 11.50$ Å. Between 5000 time steps (for the largest model) and 20 000 time steps (for the smallest model) were used for production runs. The structure was controlled by calculating partial pair-correlation functions, bond-angle distributions, and bond-angle correlation functions.

Figure 1 shows the powder-diffraction data for series of rational approximants compared with the experimental data[45] for the Frank-Kasper phase (= 1/1 approximant) and the quasicrystal. In the series of higher-order approximants, the scattering intensity converges rapidly to that measured for the i phase. The same conclusion results from a comparison of the pair-correlation functions.[26]

In a quasicrystal, any atom is found in a very large number of different environments (at least if the range

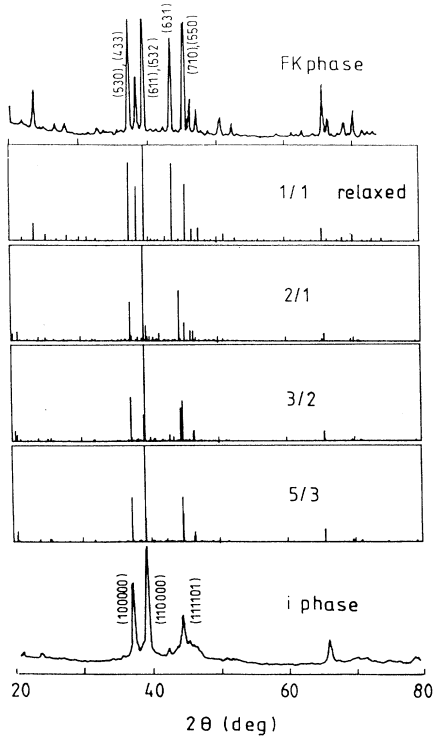

FIG. 1. X-ray powder diffraction patterns for the 1/1, 2/1, 3/2, and 5/3 rational approximants of (Al,Zn)Mg, compared with observed scattering intensities of the Frank-Kasper and the icosahedral phases (Ref. 45).

of interaction is extended far enough). Hence the interatomic forces will lead to a displacive modulation of the idealized models. A modulated tiling is a quasiperiodic structure in which the positions of the atoms can be described as positions in a tiling and displacements such that the displacement field has the same symmetry as the tiling itself (or, more precisely, the displacement field has Fourier components belonging to the Fourier module of the tiling[46]). The results of the molecular-dynamics relaxations show that for a series of higher-order crystalline approximants the displacements induced by realistic interatomic forces conserves the symmetry of the model and improves the agreement with the observed pair-correlation functions and diffraction patterns compared to earlier modeling studies based on idealized tiling models. The effect of the relaxation on the structure of 5/3 approximant is demonstrated in Fig. 2. Part (a) of the figure shows a projection of the ideal structure on the (x, y) plane, part (b) the same projection for the relaxed model. It is demonstrated that the displacive modulation of the lattice conserves the symmetry.

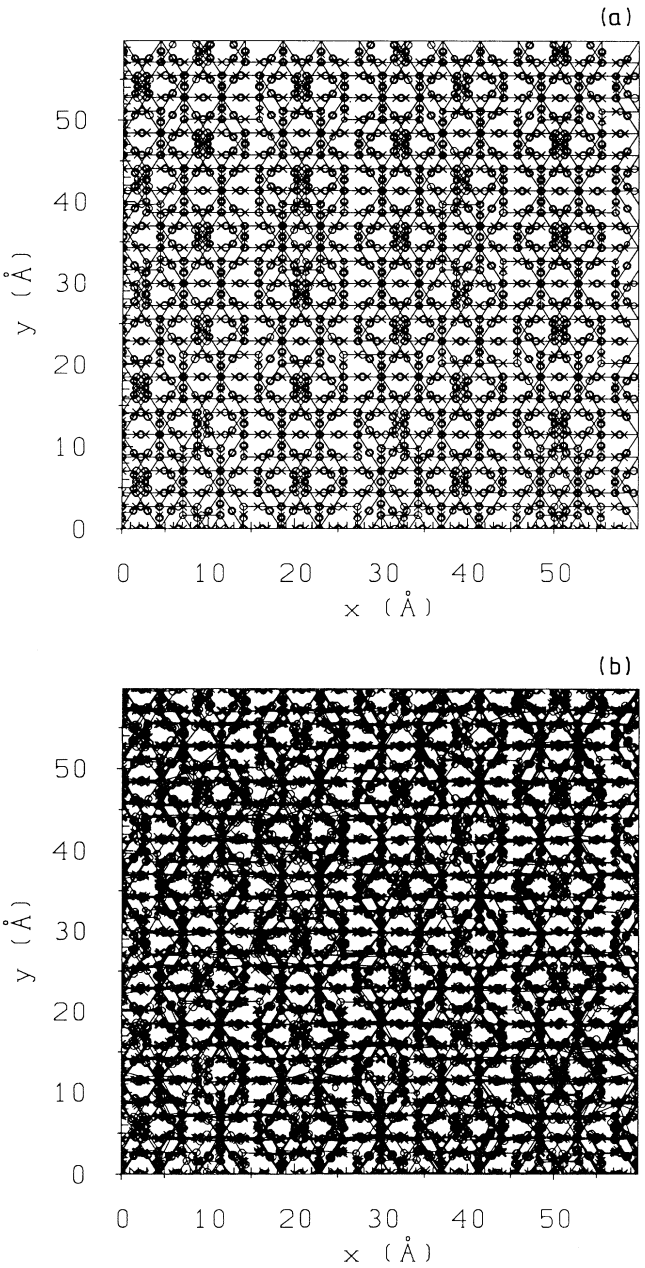

FIG. 2. Projection of the nonrelaxed structure of the 5/3 approximant on the (x, y) plane (a) and a projection of the same model after the relaxation (b).

D. Molecular-dynamics simulations of liquid and amorphous phases

The structural models of liquid and amorphous Al-Zn-Mg phases were prepared using molecular-dynamics simulation. We used the 3/2 approximant (2920 atoms in the cubic cell) as the initial configuration, heated the system up to 2000 K, and equilibrated over 5000 time steps. The pair-correlation function and structure factor exhibit the form typical for liquids. In order to obtain a model of the amorphous phase the system was quenched in 30 000 time steps to 300 K. This corresponds to a cooling rate of about 10^{14} K s^{-1}. The total (neutron weighted) structure factors $S(\mathbf{k})$ of the liquid and amorphous alloys are shown in Fig. 3. The important point is the existence of a sharp first diffraction peak at $|\mathbf{K}_p| \approx 2\pi/d$, where d is an average nearest-neighbor distance. The amplitude of this peak is a measure for the short-range order existing in the liquid or glassy phase.

III. TB-LMTO RECURSION CALCULATION OF THE ELECTRONIC STRUCTURE

On present computers fully self-consistent band-structure calculations are feasible for elementary cells with up to 100 atomic sites. Hence even the 2/1 approximant cannot be treated using **k**-space techniques. However, the electronic density of states for larger systems can be calculated in **r** space using more approximate methods, such as the recursion technique.[37,38] The recursion method is applicable to any Hamiltonian which

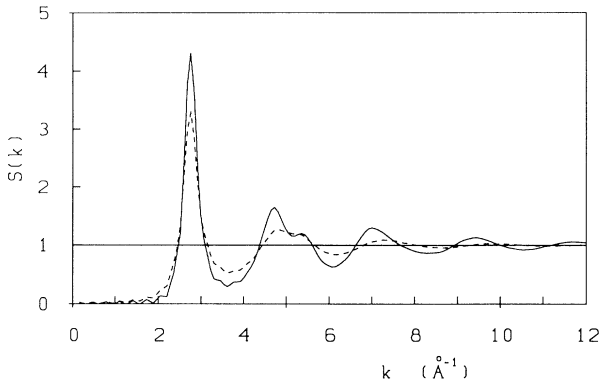

FIG. 3. Structure factors $S(\mathbf{k})$ for liquid (T=2000 K, dashed line) and amorphous (T=300 K, solid line) Al-Zn-Mg phases.

is quadratic in the dynamical variables. The calculation of the electronic structure using the recursion method may be conveniently carried out by transforming from the basis of linear muffin-tin orbitals (LMTO) to a tight-binding (TB) representation.[35,36,47]

A. TB-LMTO formalism

The two-center tight-binding Hamiltonian in the Löwdin orthonormal representation may be written[35,36] as (a superscript γ defines quantities calculated in a nearly orthonormal basis)

$$H^\gamma = \epsilon_\nu + h^\gamma, \tag{1}$$

where ϵ_ν is the reference energy for the linearization of the MTO's with the quantum number ν, where $\nu = nlm$ is a shorthand notation for the principal, angular momentum, and magnetic quantum number. The Hamiltonian (1) is accurate up to second order in $(E - \epsilon_\nu)$. The Hamiltonian matrix h^γ may be determined from the expansion (a superscript α defines quantities calculated in the screened, most localized TB basis)

$$h^\gamma = h^\alpha - h^\alpha o^\alpha h^\alpha + h^\alpha o^\alpha h^\alpha o^\alpha h^\alpha - \cdots, \tag{2}$$

where o^α is an overlap parameter and where the Hamiltonian h^α satisfies the relation

$$H^\alpha = \epsilon_\nu + h^\alpha = c^\alpha + \sqrt{d^\alpha} S^\alpha \sqrt{d^\alpha}, \tag{3}$$

where c^α and d^α are diagonal matrices of screened potential parameters describing the center of gravity and the width of each band, respectively, and S^α is a matrix of screened structure constants determined by the screening constants α. H^α is accurate to first order in $(E - \epsilon_\nu)$. The screened structure constants are given in terms of conventional LMTO structure constants S^0 by the relation

$$S^\alpha = S^0(1 - \alpha S^0)^{-1}. \tag{4}$$

Values of the screening constants providing the most localized structure constants were found from numerical studies[35,36] as $\alpha = (0.348\,48, 0.053\,030, 0.010\,714)$ for s, p, and d orbitals. When the potential parameters $C \equiv c^\gamma$, $\Delta \equiv d^\gamma$, and γ are known, the screened potential parameters c^α, d^α, and the overlap parameters o^α can be obtained using the expression[31,47]

$$\frac{c^\alpha - \epsilon_\nu}{c^\gamma - \epsilon_\nu} = \left(\frac{d^\alpha}{d^\gamma}\right)^{1/2} = \frac{\alpha - \gamma}{o^\alpha d^\gamma} = 1 + \frac{\alpha - \gamma}{d^\gamma}(c^\gamma - \epsilon_\nu). \tag{5}$$

B. Recursion calculation of density of states and spectral functions

The recursion method is a real-space method for the calculation of a diagonal element of the Green's function; the imaginary part of this matrix element gives the density of states $n_\psi(E)$ projected on an arbitrarily chosen state $|\psi\rangle$,

$$n_\psi(E) = -\frac{1}{\pi}\mathrm{Im}\langle\psi|(E + i0^+ - H)^{-1}|\psi\rangle. \tag{6}$$

If the state $|\psi\rangle$ is represented in a TB basis by a vector $u_0^{\nu,\mathbf{R}}$,

$$u_0^{\nu,\mathbf{R}} \sim \exp(i\delta_{\nu,\mathbf{R}}), \tag{7}$$

where $\delta_{\nu,\mathbf{R}}$ are uniformly distributed random numbers from the interval $[0, 2\pi)$, the resulting density of states is the total density of states, $n(E)$. A possible statistical error introduced by this random sampling may be minimized by averaging over several randomly phased vectors. If the state $|\psi\rangle$ represented by a vector $u_0^{\nu,\mathbf{R}}$ is chosen as a plane wave propagating in a direction $\mathbf{k}$,

$$u_0^{\nu,\mathbf{R}} \sim \exp(i\mathbf{kR}), \tag{8}$$

the resulting projected density of states is the Bloch spectral function $f(\mathbf{k}, E)$.

From the numerical point of view the recursion method is essentially a method for transforming a symmetric matrix into a tridiagonal form. The Green's function and the projected density of states may be expressed in a continued-fraction representation. The continued fraction may be terminated at a level $LL \ll N$ much smaller than the dimension N of the Hamiltonian matrix. The information about the spectrum of Hamiltonian eigenvalues contained in the first LL recursion coefficients is equivalent to the information contained in $2LL$ moments of the spectrum. For most of the applications $LL \sim 20$–50 is sufficient and a smooth density of states or spectral function may be obtained using a proper terminator.[37] Increasing the number of recursion levels LL over a cer-

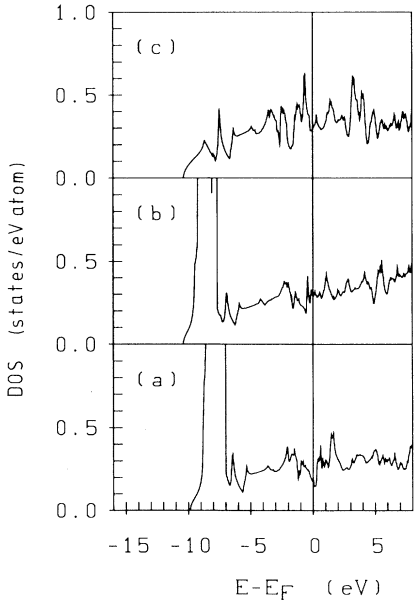

FIG. 4. Electronic density of states of the $C15$ Laves phases for different compositions: (a) Zn_2Mg, (b) $AlZn_3Mg_2$, and (c) Al_2Mg.

tain limit does not improve the resolution as problems with boundary conditions arise.

IV. ELECTRONIC STRUCTURE OF CRYSTALLINE ALLOYS AND OF THE RATIONAL APPROXIMANTS

In the following section we describe the results of self-consistent **k**-space LMTO-ASA calculations for the crystalline Frank-Kasper phase $(Al,Zn)_{49}Mg_{32}$ and for the closely related Laves phases Zn_2Mg, $AlZn_3Mg_2$, and Al_2Mg and **r**-space TB-LMTO recursion calculations for the higher-order rational approximants.

A. Laves phase

The most simple crystal structure related to the atomic arrangment in the icosahedral (Al,Zn)Mg phase is the cubic $C15$ ($MgCu_2$-type) Laves phase.[48] The rhombohedral unit cell of the $C15$ structure is just a slightly distorted PR, decorated as proposed by Henley and Elser.[25] For the $C15$ structure the electronic eigenvalues were calculated self-consistently at 505 **k** points in the irreducible part of the Brillouin zone. The density of states was calculated using the linear tetrahedron method.[49]

The calculations have been performed for the compositions Zn_2Mg, $AlZn_3Mg_2$, and Al_2Mg. For Zn_2Mg the Fermi level falls into a deep minimum of the DOS induced by a strong Bragg peak of the $C15$ lattice (Fig. 4). Upon substitution of Zn by Al, the general form of the DOS is unchanged, but the Fermi level is shifted into a region of higher DOS with increasing band filling. Experimentally, Zn_2Mg forms a stable phase crystallizing in the $C14$ ($MgZn_2$-type) Laves phase. The $C14$ and $C15$ structures are only different stacking variants of the same basic layers.[48] $C14$-$MgZn_2$ has also a deep DOS minimum at E_F (see Ref. 50), the relative stability of different Laves stacking variants may be related to the band-filling

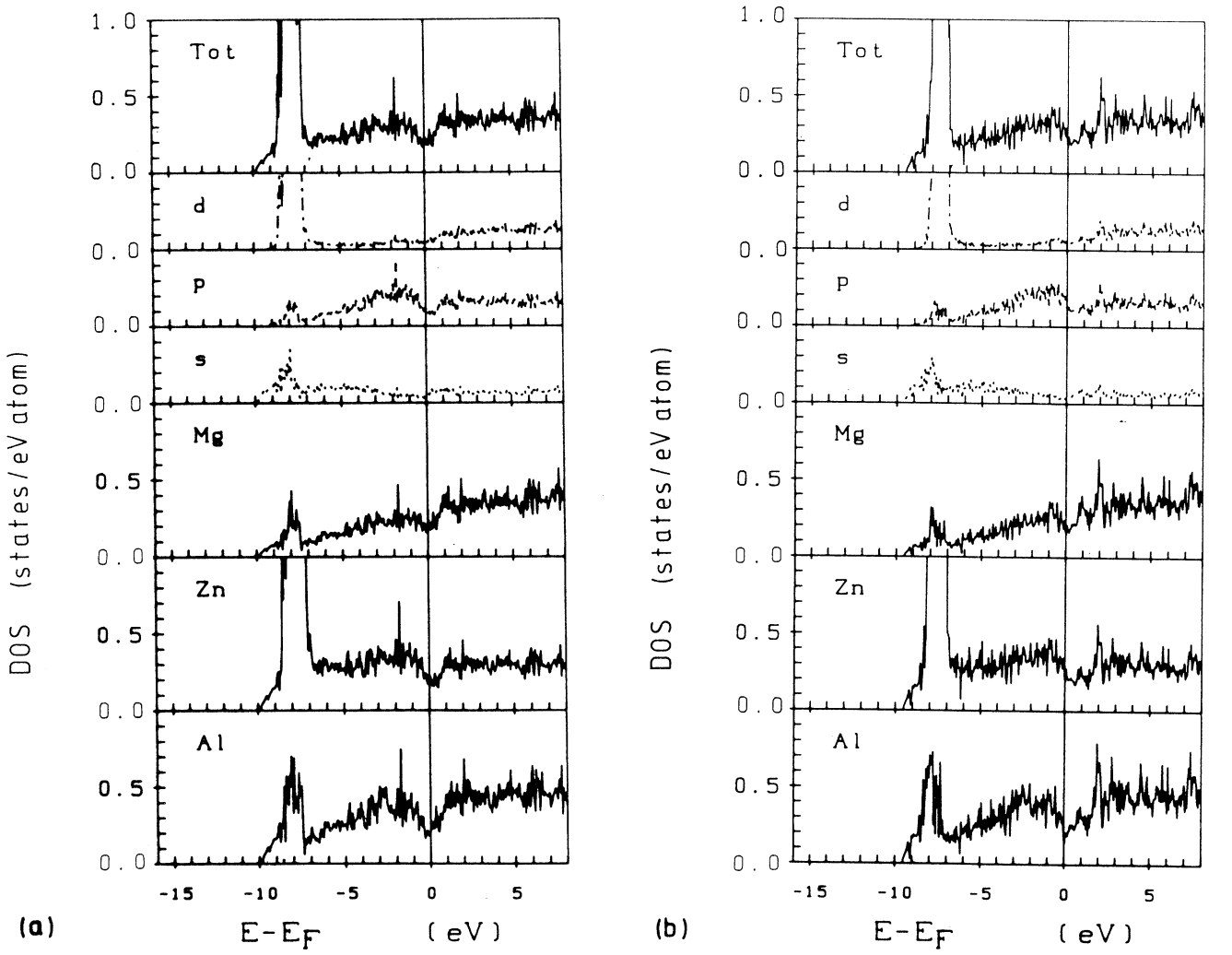

FIG. 5. Total, site, and angular momenta decomposed electronic density of states of (a) the relaxed and (b) the ideal Al-Zn-Mg Frank-Kasper phases, i.e., 1/1 approximant calculated using LMTO-ASA method. The result is obtained using 55 **k** points.

Hume-Rothery-type argument.[51,52] As the possible Laves phase stacking variants have identical first-, second-, and third-neighbor shells, the first four moments of the DOS are equal. According to a theorem of Ducastelle and Cyrot-Lackmann,[53] the structural energy difference between two structures whose first m moments of the DOS are equal has at least $(m-1)$ moments between the end points of an empty and a full band. This leads to the oscillatory dependence of phase stability on the band filling (for more detailed discussion, see Ref. 52). With gradual substitution of Zn by Al, the overall structure of the valence band is unchanged (except close to the bottom of the band where the *s-d* hybridization causes a broadening of the bandwidth in Zn_2Mg over the free-electron value, whereas the width in Al_2Mg is almost exactly free-electron-like). With increasing band filling, the Fermi level is shifted out of the structure-induced minimum, so that a mixed $(Al,Zn)_2Mg$ Laves phase and a hypothetical Al_2Mg phase receive only very little band-gap stabilization.

B. Frank-Kasper phase

The electronic eigenvalues for the Frank-Kasper phase $Al_{13}Zn_{36}Mg_{32}$ (the 1/1 approximant of the *i* phase) were calculated using the LMTO-ASA method. The bcc symmetry of this approximant allows one to reduce the number of atoms to 81 atoms in the primitive cell. For the electronic structure calculations, the Al atoms are placed on the vertices, the Zn atoms on the midedge positions of all structural units.[25] This decoration leads to an approximately correct chemical composition of the Frank-Kasper phase. The Henley-Elser decoration defines a set of idealized atomic coordinates. The MD relaxation changes the coordinates without breaking the symmetry of the lattice. The relaxed coordinates are in good agreement with those measured by Bergman, Waugh, and Pauling.[24] Details of the crystallographic description for idealized, relaxed, and observed structures are given in Ref. 26.

We used 55 **k** points in the irreducible wedge of the Brillouin zone. The integration over the Brillouin zone and the calculation of the density of states was performed using the tetrahedron method. The position of the reference energies ϵ_ν was determined from the zero-moment condition.[32] The potential parameters C, Δ, and γ were determined self-consistently for each atomic site.

The self-consistent DOS of the Frank-Kasper phase is shown in Fig. 5; part (b) refers to the ideal structure, part (a) to the MD relaxed lattice where each atom sits in the equilibrium position. The dominant feature of the DOS is the sharp peak of Zn 3*d* states near the bottom of the band. At the Fermi energy, the DOS shows a broad, deep minimum induced by the closely spaced (631), (710)+(550), and (640) reciprocal-lattice vectors of the cubic Frank-Kasper phase. We note that these lattice vectors correspond to the (111101) Bragg reflection of the icosahedral phase (cf. Fig. 1). The calculated DOS at the Fermi energy is $n(E_F) = 0.17$ states/(eV atom), it is significantly lower than the free-electron DOS $[n(E_F) = 0.36$ states/(eV atom)] and also some-

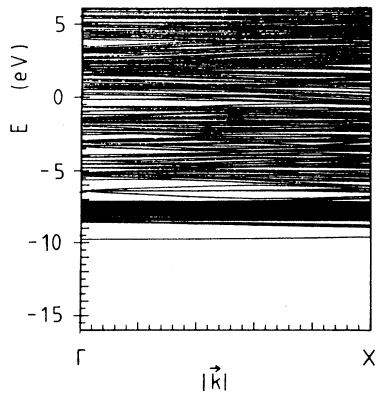

FIG. 6. Electronic dispersion relations of the Al-Zn-Mg Frank-Kasper phase calculated along the Γ-X direction.

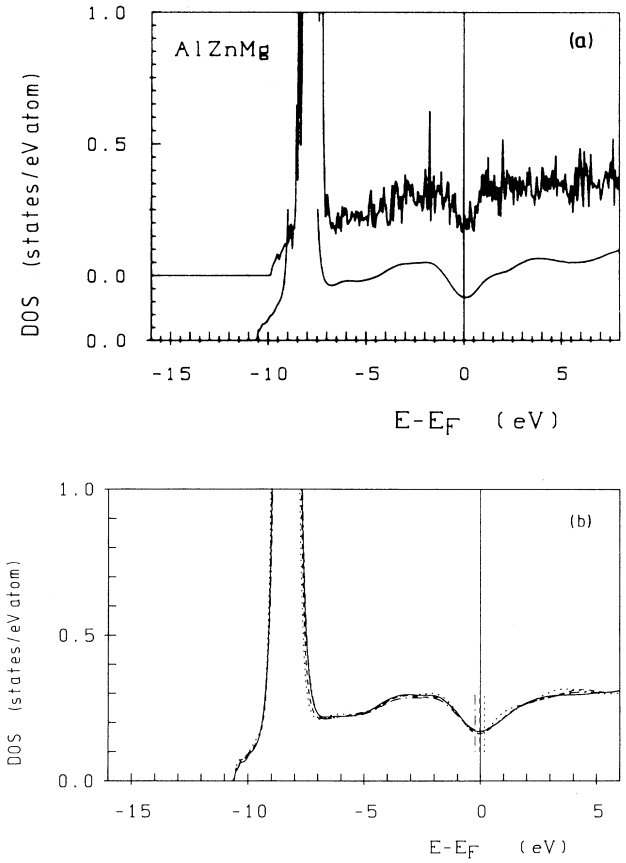

FIG. 7. (a) Electronic density of states for the 1/1 approximant calculated using the **k**-space LMTO method for 55 **k** points and using the **r**-space TB-LMTO and recursion methods (smooth curve). (b) Electronic density of states for 1/1 (dotted curve), 2/1 (dashed curve), 3/2 (dot-dashed curve), and 5/3 (solid curve) crystalline approximants (with 162, 688, 2920, and 12 380 atoms, respectively), calculated using the real-space TB-LMTO recursion method.

what lower than the experimental values of Graebner and Chen[54] [$n(E_F) = 0.30$ states/(eV atom)] and of Mizutani *et al.*[27] [$n(E_F) = 0.33$ states/(eV atom)]. The difference probably has to be attributed to the Al(Zn) substitutional disorder in the real Frank-Kasper phase that has been neglected in our calculation.

The global shape of the DOS may be described as a free-electron-like parabolic band modulated by the van Hove singularities of the complex crystal structure. Studies of the electronic spectrum of 1D and 2D models of quasicrystals[3–5] show that the spectrum is singular continuous. The spiky structure of the DOS of the 1/1 approximant calculated using the supercell LMTO-ASA method allows us to conjecture that the DOS for 3D infinite quasicrystals will be strongly structured, though not necessarily singular continuous. The spiky character of the spectrum seems to be also experimentally confirmed: The transport properties of quasicrystalline samples are extremely sensitive to their composition and hence to the position of the Fermi level.[55] In Figs. 5(a) and 5(b) we compare the DOS's calculated on the idealized and on the relaxed Frank-Kasper lattice. The atomic relaxation affects the electronic structure only at a local level. In the idealized structure, there are six short Mg-Mg distances in the cubic cell. These short distances are the vertex-to-vertex distances in the hexagonal bipyramid inside the rhombic dodecahedra. These short distances generate localized states centered in the short bonds, at energies far below the bottom of the valence band [$(E - E_F) = -24.7$ eV]. For these states convergence could be reached only by fixing the reference energy ϵ_ν close to the Fermi level. Relaxation causes an elongation of the hexagonal bipyramid, and the relaxed Mg-Mg distances are of the proper length. No localized states below the bottom of the valence band exist in the relaxed Frank-Kasper phase. The relevant DOS close to the Fermi energy is hardly affected, except for a slight shift of the DOS minimum to lower energies. This shift expresses the effect of an energetically more favorable arrangement of the ions, $n(E_F) = 0.17$ states/(eV atom), for both the ideal and relaxed structure.

Figure 6 shows the dispersion relations for the electronic eigenvalues along the Γ-X direction. All bands show only very weak dispersion. At the zone boundary, the spectrum is quasicontinuous, but relatively broad symmetry-induced gaps exist at the Γ point. Close to the Fermi energy these gaps extend from Γ to the Brillouin-zone boundary.

C. Higher-order approximants

The basis for the construction of the TB Hamiltonian for the higher-order approximants is the self-consistent LMTO-ASA supercell calculation for the crystalline 1/1 approximant. We transfer the potential parameters obtained from the supercell calculation for the 1/1 approximant to the larger approximants in the following way: We take the average of the potential parameters over equivalent sites. We consider three different sites: vertex positions occupied by Al atoms, midedge positions occupied by Zn atoms, and Mg positions inside prolate

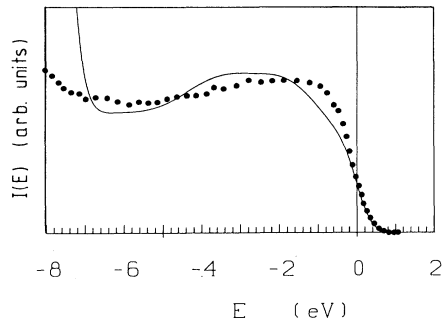

FIG. 8. Comparison of the DOS of the 5/3 approximant to quasicrystalline Al-Zn-Mg phase (solid line) with the photoemission results (dots) (after Ref. 57).

rhombohedra and inside rhombic dodecahedra. For the sake of simplicity we did not distinguish between different Mg positions inside the rhombic dodecahedron. We verified for the 1/1 approximant that the averaging of the potential parameters had negligible effect on the resulting density of states. Atomic sites in the larger approximants were decorated by the averaged potential parameters.

The screened structure constants were calculated using Eq. (4) by matrix inversion for each atomic site. The structure constants were calculated including all neighbors within a sphere of radius $R_{\rm cut} = 2.7R_{\rm WS}$ ($R_{\rm WS}$ is the Wigner-Seitz radius). The expansion (2) was truncated at the third order. Using a second-order expansion only led to an insufficient accuracy of the DOS around E_F. We verified that using a fourth-order expansion in Eq. (2) improved the DOS only negligibly in the region of interest.

We calculated the density of states and the spectral function for the entire sequence of approximants starting from the 1/1 to the 5/3 approximant. We combined 27 and 8 elementary cells to a supercell for the 1/1 and 2/1 approximants, respectively. The density of states

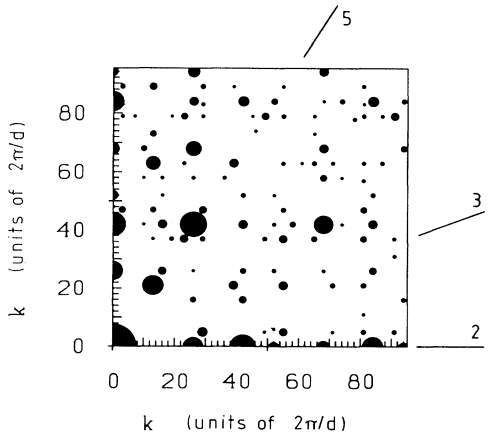

FIG. 9. Diffraction pattern for the 5/3 approximant to i-Al-Zn-Mg in a plane perpendicular to a twofold axis. The direction of the twofold, threefold, and fivefold symmetry axes is marked. The wave vector $|\mathbf{k}|$ is given in units of $(2\pi/d)$, where d is the period of the approximant, $d = 59.82$ Å.

was calculated using the Gaussian quadrature[56] from 50 recursion levels. The Bloch spectral function was calculated by the Luchini-Nex terminator[57] using 40 exact recursion levels. The finite size of the supercell limits the number of recursion levels. The truncation of the continued fraction at a finite level leads to a finite resolution of the calculated DOS. For 50 recursion levels and a bandwidth of $\sim$ 10 eV, the estimated resolution is $\sim$ 0.2 eV. As a consequence the spiky fine structure of the DOS is smoothed out.

1. Density of states

The comparison of DOS of the 1/1 approximant calculated using the self-consistent LMTO-ASA method with that calculated by the TB-LMTO recursion method

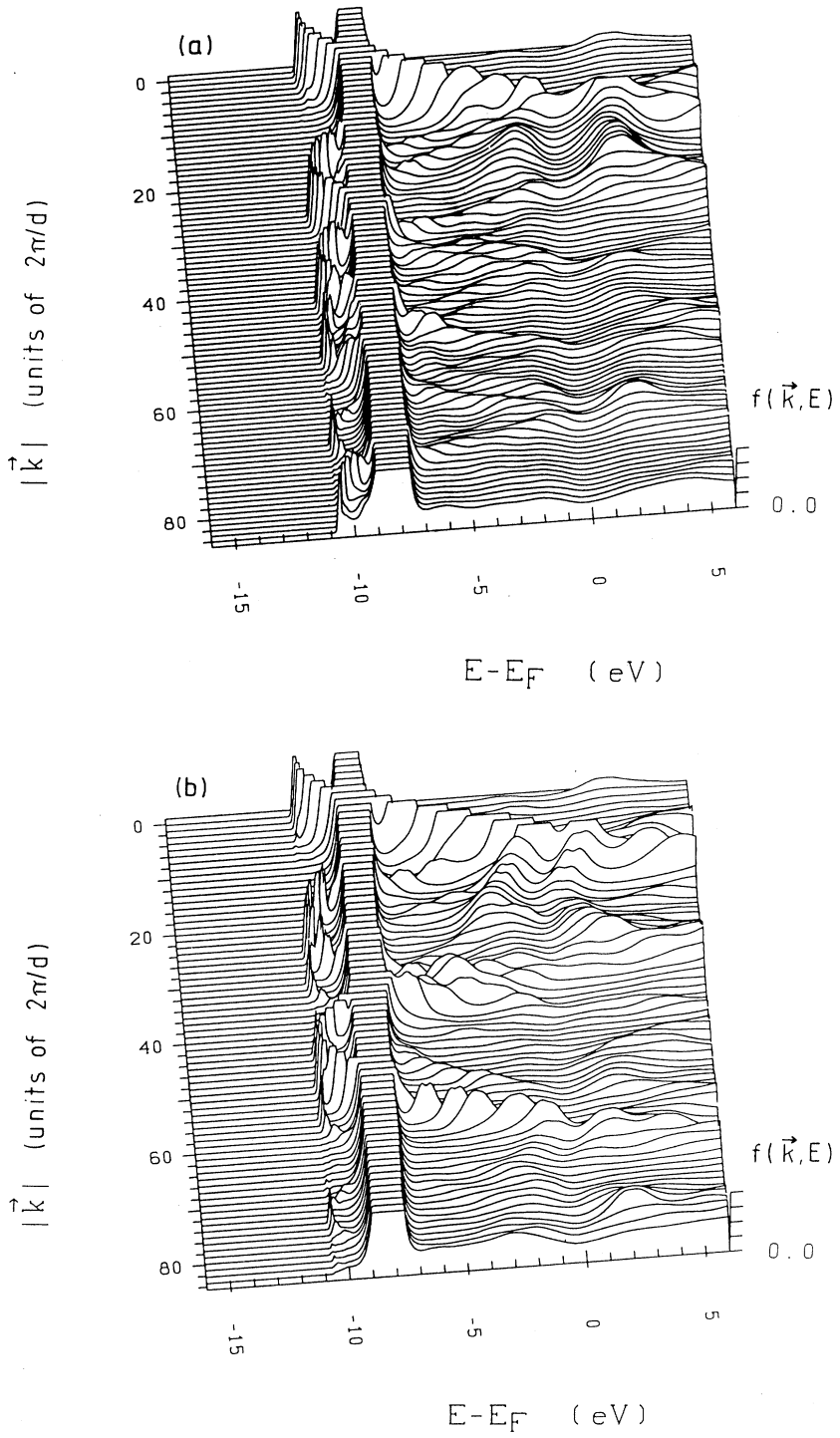

FIG. 10. Bloch spectral function $f(\mathbf{k}, E)$ calculated using the recursive method for wave vectors pointing along (a) a twofold and (b) a fivefold (b) axis. The wave vector $|\mathbf{k}|$ is given in units of $(2\pi/d)$, where d is the period of the approximant.

[Fig. 7(a)] shows that the recursion method reproduces the overall structure of DOS very well. The fine structure is, of course, not reproduced in the recursion results. Particularly interesting is the behavior of the DOS around the Fermi level. We observe here a deep minimum in the DOS for all approximants [Fig. 7(b)]. The fact that the calculated DOS converges very rapidly in the sequence of the rational approximants suggests that this DOS minimum (or "pseudogap") is a generic property not only of the rational approximants, but also of the quasicrystal. As we have already mentioned in the Introduction, the rapid convergence of the electronic properties (DOS at the Fermi level, resistivity, thermopower) of the approximant crystals to the value found in the quasicrystal has also been confirmed experimentally.[30,58] The existence of the DOS minimum is also confirmed by photoemision spectroscopy. Figure 8 compares the calculated DOS for the 5/3 approximant with the photoemission results of Tanaka.[59] The form of the valence band and the depth of the pseudogap are in good agreement with the x-ray-photoemission-spectroscopy (XPS) spectrum. The appearent position of the Zn $3d$ band in the photoemission intensity is shifted to higher binding energy relative to the position observed in the DOS. This effect is well understood in terms of the screened self-interaction of the hole in the narrow $3d$ band (cf. Ref. 50 for a more detailed discussion).

The origin of the DOS minimum is often discussed in terms of a Fermi-surface–Brillouin-zone interaction. We think that this argument does not consider the essential effect of quasiperiodicity: Icosahedral symmetry allows for a more spherical Brillouin zone, and the intersection of a spherical Fermi surface with a nearly spherical Brillouin zone can lead to a disappearence of a large part of the nearly-free-electron Fermi surface. However, this argument assumes that the higher zones may be (at least approximately) folded down in $\mathbf{k}$ space. Hence the argument accounts for the effect of icosahedral symmetry, but ignores the influence of quasiperiodicity. This can be explored only if we investigate the energy-momentum relation in an extended region of $\mathbf{k}$ space.

2. *Bloch spectral functions and quasiperiodic dispersion relations*

It has been pointed out[9] that for each hypercubic 6D lattice L_6, there exists a 6D reciprocal lattice. A 3D

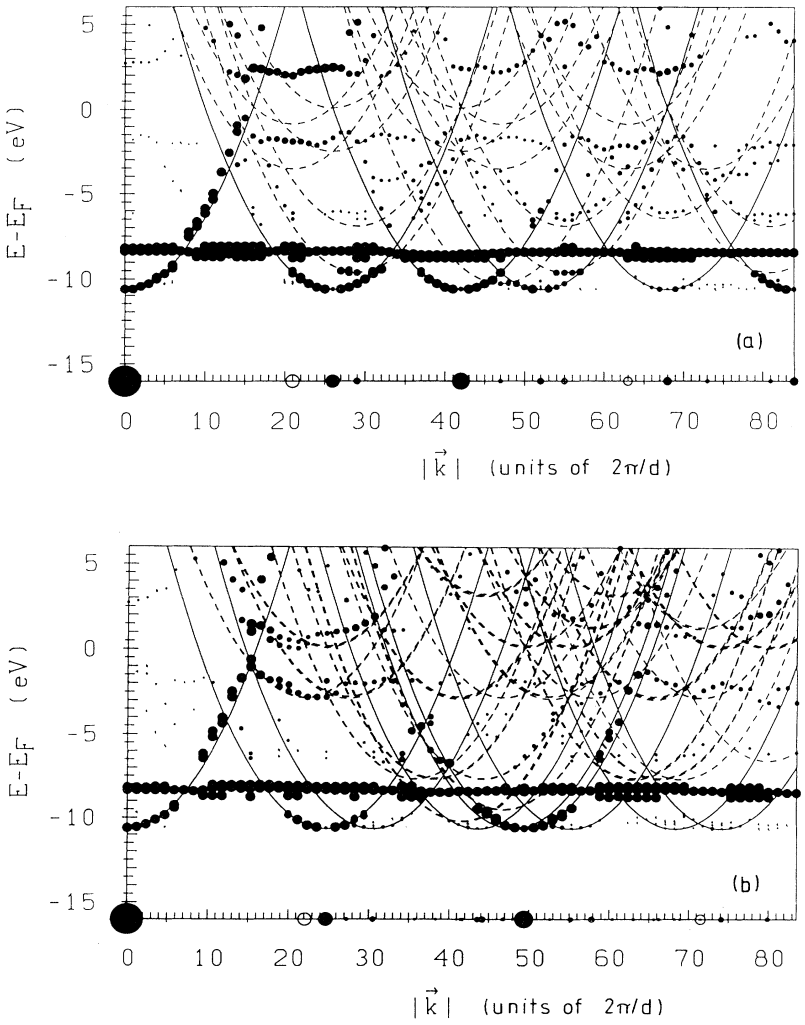

FIG. 11. Dispersion relation $E(\mathbf{k})$ derived from maxima of the Bloch spectral functions for wave vectors pointing along (a) a twofold and (b) a fivefold (b) axis. The wave vector $|\mathbf{k}|$ is given in units of $(2\pi/d)$, where d is the period of the approximant. The solid circles on the $\mathbf{k}$ axis represent Γ points on the symmetry axis. They give rise to parabolic dispersion relations originating from the bottom of the band and shown by full parabolas. The open circles represent projections of the Γ points off the symmetry axis. The dashed lines show the parabolic dispersion surfaces originating from these points.

reciprocal lattice for the quasicrystal is defined by a projection of this 6D reciprocal lattice on 3D space. Special points of the 3D reciprocal quasilattice are projections of high-symmetry points of the 6D reciprocal lattice of the hypercubic crystal. Special points are characterized by a generalized structure factor.[9] Of particular interest are the Γ points, i.e., the projections of the (000000) points of the hypercubic lattice reciprocal to L_6. In this case the generalized structure factor reduces to the conventional structure factor.

Figure 9 shows the calculated diffraction pattern for the 5/3 approximant to i-AlZnMg in a plane perpendicular to a twofold axis and containing twofold, threefold, and fivefold symmetry axes. The size of each diffraction spot is scaled with the calculated intensity. The most intense diffraction peaks are the dominant Γ points of the quasilattice. In principle, the Γ points are distributed densely in $\mathbf{k}$ space. However, only a discrete set of points has a sufficiently large spectral weight.

Figure 10 shows the Bloch spectral functions $f(\mathbf{k}, E)$, calculated using the recursive method for wave vectors pointing along the twofold and fivefold symmetry directions. For a crystal, a δ-function peak in the spectral function defines an eigenvalue for the given $\mathbf{k}$ vector. As translational symmetry is broken, the spectral function of a quasicrystal is a smooth curve (again with a finite resolution arising from the truncation of the continued fraction). A peak in $f(\mathbf{k}, E)$ at the energy E_0 represents an *approximate* eigenstate with a wave vector $\mathbf{k}$ and energy E_0. The width of the peak is inversely proportional to the lifetime of the state. We find from Fig. 10 that the spectral functions of the Al-Zn-Mg quasicrystal consists of a dispersionless (i.e., $\mathbf{k}$-independent) peak near $E = -8$ eV representing the localized Zn $3d$ orbitals [the peaks in Figs. 10(a) and 10(b) are truncated above the value 0.04] and a sequence of parabolic bands originating from a discrete set of $\mathbf{k}$ points (the Γ points of the reciprocal quasilattice). Electronic dispersion relations defined in terms of peaks in the Bloch spectral functions are drawn in Fig. 11. Every Γ point is the origin of a nearly parabolic (s,p) valence band (note that there are also Γ points off the symmetry axis giving rise to shifted parabolic bands). The amplitude of the peak in the spectral function depends on the weight of the Γ point. For comparison, the parabolic dispersion relations of a quasiperiodic nearly-free-electron model are shown. The existence of sharp peaks in the Bloch spectral functions shows that propagating electronic states exist in the vicinity of the quasiperiodic Γ points.

The difference from the extended zone scheme of a crystal is that in the icosahedral phase the Γ points are distributed quasiperiodically; hence, the electronic dispersion relations are also quasiperiodic. Close to the Fermi energy we find a series of highly degenerate free-electron states at quasiperiodically spaced wave vectors. The planes normal to these wave vectors define the analog of a Brillouin zone in the extended zone scheme of a crystal. Because of the icosahedral symmetry, these "quasi-Brillouin-zones" have many faces and are nearly isotropic. The electron-ion interaction lifts the degeneracy of the free-electron states and leads to the formation of a pseudogap confined between two bands with almost no dispersion. The important point is that the pseudogap is found at all wave vectors. The comparison of the results calculated for the twofold and fivefold directions shows that at low energies the dispersion relations are isotropic and that the pseudogap exists in all symmetry directions. Hence the Fermi velocity of the electrons will be low, independent of the direction in which the electrons propagate.

V. ELECTRONIC STRUCTURE OF LIQUID AND AMORPHOUS ALLOYS

The origin of the pseudogap at the Fermi level may be better understood if we compare the DOS of an approximant to the quasicrystal with the DOS of related aperiodic phases. In Fig. 12 we compare the DOS of the 3/2 approximant to a Al-Zn-Mg quasicrystal, with the DOS of the same system in liquid and amorphous phases. We note that the 3/2 approximant in the Al-Zn-Mg system was recently observed experimentally.[60] The preparation of the structural models of liquid and amorphous systems is described in Sec. II D. The DOS was calculated using the TB-LMTO recursion method. The energy scales in Fig. 12 are aligned to match the bottom of the valence band. We find an almost perfect parabolic free-electron band for liquid Al-Zn-Mg, while for the amorphous phase a shallow minimum around the Fermi level is predicted. As the systems have the same chemical composition, it is evident that the origin of the pseudogap at the Fermi level in the DOS of the approximant to the quasicrystal and obviously also the shallow minimum around the Fermi level on the DOS of amorphous phase have no chemical origin, but they are *structure induced.*

The comparison of the corresponding Bloch spectral functions is presented in Fig. 13. While for the spectral function of the liquid only one free-electron-like s,p

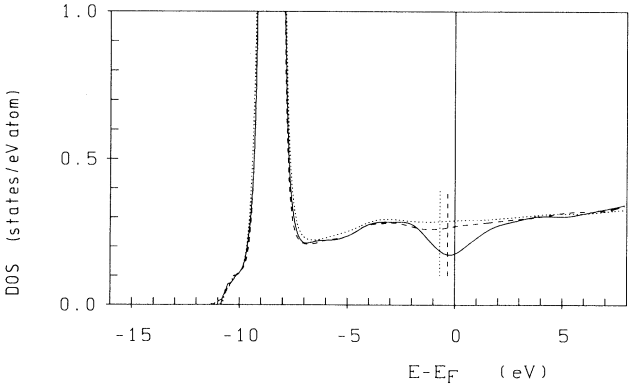

FIG. 12. Comparison of the DOS of the 3/2 approximant to i-Al-Zn-Mg (solid line) with the DOS of the same system in the liquid (dotted line) and amorphous (dashed line) phases. The energy scales are aligned to match the bottom of the bands. The Fermi level is marked by vertical line segments.

parabolic band with origin at $\mathbf{k} = 0$ is seen [Fig. 13(a)], for the amorphous phase a weak indication for a second parabolic band with the origin at $\mathbf{k} = \mathbf{K}_p$ is observed [Fig. 13(b)]. This band is induced by the first peak in the structure static factor at $|\mathbf{K}_p|$. It is sharper and higher for the amorphous phase than for the liquid phase (see Fig. 3). The shallow minimum of the DOS at the Fermi level of the amorphous phase is induced by the same mechanism as the pseudogap at E_F in the crystalline and quasicrystalline phases. The sharp first peak in the static structure factor acts like a smeared-out reciprocal-lattice vector. Hence there exists a low-intensity parabolic band originating from $|\mathbf{k}| = |\mathbf{K}_p|$, and the two free-electron bands are degenerate at $|\mathbf{k}| = |\mathbf{K}_p/2|$. Lifting of the degeneracy leads to the formation of a shallow isotropic pseudogap.

VI. HUME-ROTHERY MECHANISM FOR THE STABILITY OF QUASICRYSTALS

Our results show that structure-induced pseudogaps in the electronic DOS at the Fermi level exist in rational approximants to quasicrystals, but also in related crystalline and amorphous alloys. Hence we are led to con-

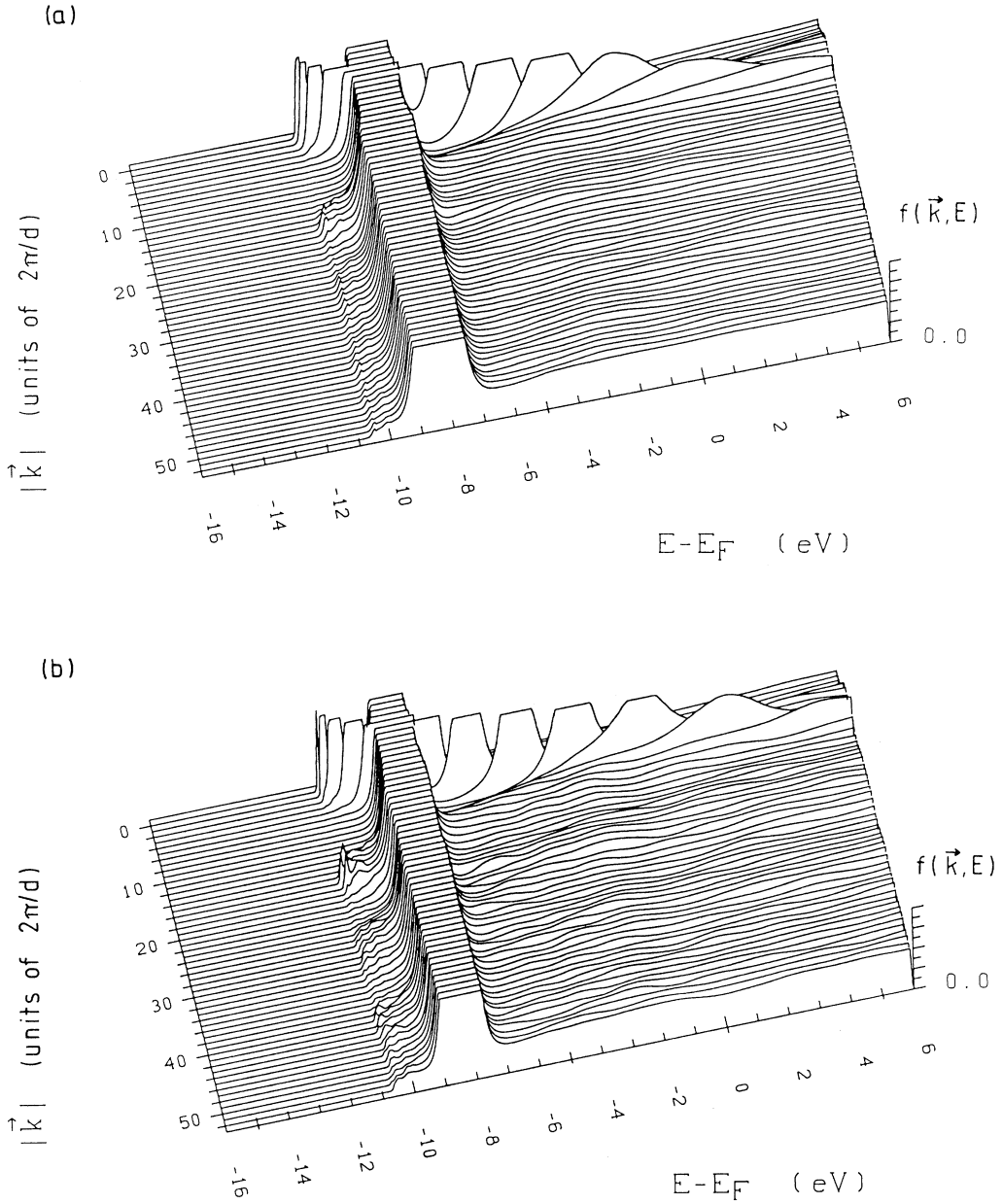

FIG. 13. Bloch spectral functions $f(\mathbf{k}, E)$ for (a) the liquid, (b) the amorphous phase, and (c) the 3/2 approximant along a twofold axis. The wave vector $|\mathbf{k}|$ is given in units of $(2\pi/d)$, where d is the period of the 3/2 approximant, $d = 36.97$ Å.

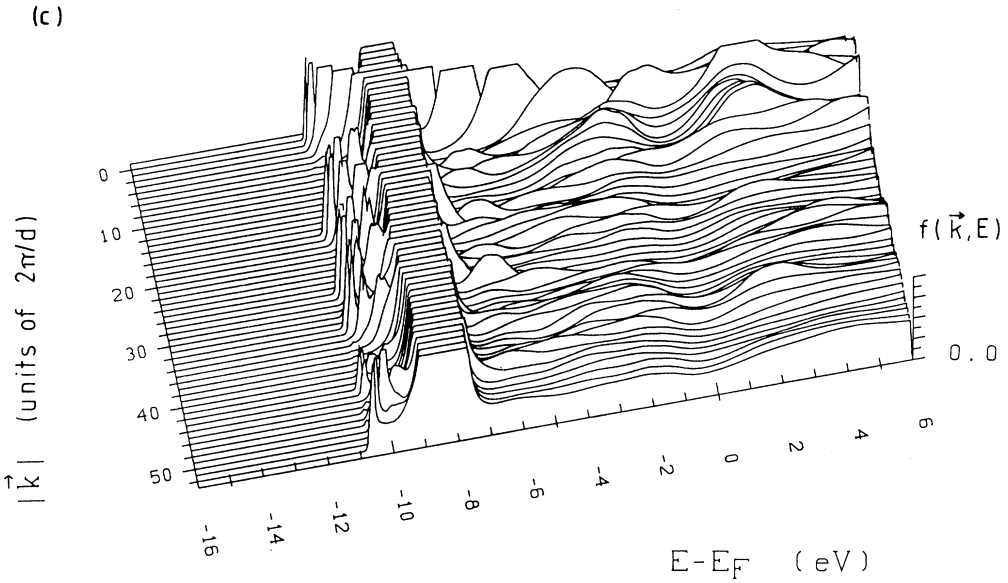

FIG. 13. (*Continued*).

clude that although existence of a pseudogap is probably a generic property of quasicrystals, but is not a specific property that distinguishes quasiperiodic from periodic or aperiodic alloys. The problem is a quantitative rather than qualitative one.

The stabilization effect of the pseudogap at the Fermi level in the DOS may be estimated from the comparison of the total energies of an approximant to the quasicrystal with the amorphous phase. Such a comparison is physically meaningful as the Al-Zn-Mg quasicrystal is prepared by the rapid quenching technology and hence the competing phase to the icosahedral phase is just the amorphous phase. The difference in total energies of the systems may be calculated using the local force theorem.[61] Both systems have the same chemical composition and the same volume, and therefore the difference in the total energies may be well approximated by the difference in one-electron energies. We find that the energy of the 3/2 approximant is lower by $\Delta U = 27$ meV/atom.

We find no evidence for a deepening of the pseudogap with an increasing period of the approximant. For the Al-Zn-Mg alloys such a deepening is not to be expected, since the Frank-Kasper phase (the 1/1 approximant) and also the recently observed 3/2 approximant[60] are stable phases, whereas the quasiperiodic alloys are only metastable. Very recently the electronic properties of the stable Al-Cu-Li and Al-Cu-Fe quasicrystals and their body-centered-cubic and rhombohedral 1/1 approximants have been studied by nuclear magnetic resonance.[62] For *i*-Al-Cu-Li a small deepening of the pseudogap compared to the approximant was found. For the approximant, the result is in agreement with theoretical predictions.[34] For the higher-order approximants, the electronic structure has still to be calculated. After recent progress in the modeling of the atomic structure,[63] such calculations appear to be feasible.

Our results shed more light on the role of a Hume-Rothery mechanism for the stability of quasicrystals. For metastable phases such as *i*-AlZnMg, the electronic energy of the quasicrystalline and the approximant phases are nearly equal. In such a case it might be the entropy of the disordered quasicrystal which dips the balance in the free energy in favor of the quasicrystalline state. For the stable quasicrystals, an energetic stabilization appears to be possible.

VII. CONCLUSIONS

We have presented an investigation of the electronic structure of rational approximants to a quasicrystal and of related alloys. The example chosen for our study is the Al-Zn-Mg system. We have demonstrated that propagating electronic states (i.e., states with a well-defined energy–wave-vector relation) exist close to the Γ points of the reciprocal quasilattice. We have shown that pseudogaps at the Fermi energy are truly a generic property of rational approximants approaching the quasicrystalline structure very closely. Highly degenerate free-electron states at the Fermi level were found. The pseudogaps are formed by lifting the degeneracy of these states. Our study extends and confirms arguments in favor of an electronically driven stability of quasicrystals formulated in terms of pseudogaps in the electronic density of states induced by "quasi-Brillouin-zone"–Fermi-surface interactions. We have also shown that a quasiperiodic generalization of a nearly-free-electron approximation is appropriate for s,p-bonded quasicrystals such as Al-Zn-Mg.

Our results may be relevant also in the discussion of the unusual transport properties of quasicrystals. For stable quasicrystals semimetallic transport properties characterized by high resistivity and strong temperature and

composition dependencies of the thermopower and Hall coefficient were experimentally observed.[28] In our calculations we found that the dispersion relation $E(\mathbf{k})$ for states close to the Fermi level is almost independent of $\mathbf{k}$. The Fermi velocity $v_F = |\partial E(\mathbf{k})/\partial \mathbf{k}|$ at $E = E_F$ is therefore very low. From the approximate relation for the conductivity, $\sigma = e^2 \tau n(E_F) v_F^2/3$, where τ is a relaxation time, it follows that for low Fermi velocity v_F and low density of states at Fermi level $n(E_F)$ the conductivity is also low. The strong temperature and composition dependences of the thermopower and the Hall coefficient may be attributed to the spiky character of the spectrum.

ACKNOWLEDGMENTS

This work was supported by the Fonds zur Förderung der wissenschaftlichen Forschung (Austrian Science Foundation) under Project No. 8148-TEC. M.K. acknowledges support from the Institute of Physics of the Slovak Academy of Sciences in Bratislava.

*Permanent address: Institute of Physics, Slovak Academy of Sciences, CS-84228 Bratislava, ČSFR.

[1] D. Shechtman, I. Blech, D. Gratias, and J. W. Cahn, Phys. Rev. Lett. **53**, 1951 (1984).
[2] M. Gardner, Sci. Am. **236**, 110 (1977).
[3] M. Kohomoto and B. Sutherland, Phys. Rev. B **34**, 3849 (1986); **35**, 1025 (1987).
[4] T. Fujiwara, M. Kohomoto, and T. Tokihiro, Phys. Rev. B **40**, 7413 (1989).
[5] H. Tsunetsugu, T. Fujiwara, K. Ueda, and T. Tokihiro, J. Phys. Soc. Jpn. **55**, 1420 (1986).
[6] T. Fujiwara and H. Tsunetsugu, in *Quasicrystals: The State of the Art*, edited by D. P. Vicenzo and P. J. Steinhardt (World Scientific, Singapore, 1991), p. 343.
[7] H. Patel and D. Sherrington, Phys. Rev. B **40**, 11 185 (1989).
[8] J. Hafner and M. Krajčí, Phys. Rev. Lett. **68**, 2321 (1992).
[9] K. Niizeki and T. Akamatsu, J. Phys. Condens. Matter **2**, 2799 (1990).
[10] M. Krajčí and T. Fujiwara, Phys. Rev. B **38**, 12 903 (1988).
[11] C. A. Guryan, A. I. Goldman, P. W. Stephens, K. Hiraga, A. P. Tsai, A. Inoue, and T. Masumoto, Phys. Rev. Lett. **62**, 2409 (1989).
[12] P. A. Bancel and P. A. Heiney, Phys. Rev. B **33**, 7917 (1986).
[13] A. P. Smith and N. W. Ashcroft, Phys. Rev. Lett. **59**, 1365 (1987).
[14] V. G. Vaks, V. V. Kamyshenko, and G. D. Samolyuk, Phys. Lett. A **132**, 131 (1988).
[15] A. P. Tsai, A. Inoue, and T. Masumoto, Sci. Rep. Res. Inst. Tohoku Univ. Ser. A **36**, 112 (1991).
[16] J. Hafner and M. Krajčí, Europhys. Lett. **13**, 335 (1990); in *Physics and Chemistry of Finite Systems: From Clusters to Crystals*, edited by P. Jena, S. N. Khanna, and B. K. Rao (Kluwer, Dordrecht, 1992), Vol. I, p. 587.
[17] S. R. Nagel and J. Tauc, Phys. Rev. Lett. **35**, 380 (1975).
[18] J. Hafner and L. von Heimendahl, Phys. Rev. Lett. **42**, 385 (1979).
[19] S. J. Poon, Adv. Phys. **41**, 303 (1991).
[20] T. Tokihiro, T. Fujiwara, and M. Arai, Phys. Rev. B **38**, 5981 (1988).
[21] V. Elser, Acta Crystallogr. A **42**, 36 (1986).
[22] P. Bak, Phys. Rev. Lett. **56**, 861 (1986).
[23] M. Mihalkovič and P. Mrafko, J. Non-Cryst. Solids **143**, 225 (1992).
[24] G. Bergman, J. L. T. Waugh, and L. Pauling, Acta Crystallogr. **10**, 254 (1957).
[25] C. L. Henley and V. Elser, Philos. Mag. Lett. **53**, 115 (1986).
[26] M. Krajčí and J. Hafner, Phys. Rev. B **46**, 10 669 (1992).
[27] U. Mizutani, A. Kamiya, T. Fukunaga, and T. Matsuda, in *Proceedings of the China-Japan Symposium on Quasicrystals*, edited by K. H. Kuo and T. Ninomiya (World Scientific, Singapore, 1991), p. 248.
[28] K. Edagawa, K. Suzuki, M. Ichihara, S. Takeuchi, A. Kamiya, and U. Mizutani, Philos. Mag. Lett. **64**, 95 (1991).
[29] K. Edagawa, N. Naito, and S. Takeuchi, Philos. Mag. B **65**, 1011 (1992).
[30] U. Mizutani, T. Matsuda, Y. Itoh, K. Tanaka, H. Domae, T. Mizuno, S. Murasaki, Y. Miyoshi, K. Hashimoto, and Y. Yamada, J. Non-Cryst. Solids (to be published).
[31] O. K. Andersen, O. Jepsen, and D. Glötzel, in *Highlights of Condensed Matter Theory*, edited by F. Bassani, F. Fumi, and M. P. Tosi (North-Holland, Amsterdam, 1985).
[32] H. L. Skriver, *The LMTO Method* (Springer, Berlin, 1984).
[33] T. Fujiwara, Phys. Rev. B **40**, 942 (1989); J. Non-Cryst. Solids **117+118**, 844 (1990).
[34] T. Fujiwara and T. Yokokawa, Phys. Rev. Lett. **66**, 333 (1991).
[35] O. K. Andersen and O. Jepsen, Phys. Rev. Lett. **53**, 2571 (1984).
[36] M. Šob, O. Jepsen, and O. K. Andersen, Z. Phys. Chem. Neue Folge **155**, 515 (1988); O. K. Andersen, O. Jepsen, and M. Šob, in *Electronic Band Structure and its Applications*, edited by M. Yussouff, Vol. 238 of Lecture Notes in Physics (Springer, Berlin, 1987).
[37] R. Haydock, V. Heine, and M. J. Kelly, J. Phys. C **8**, 2591 (1978).
[38] V. Heine, in *Solid State Physics*, edited by H. Ehrenreich, F. Seitz, and D. Turnbull (Academic, New York, 1980), Vol. 35, p. 1.
[39] J. E. S. Socolar, P. J. Steinhardt, and D. Levine, Phys. Rev. B **32**, 5547 (1985).
[40] F. Gähler and J. Rhyner, J. Phys. A **19**, 267 (1986).
[41] J. Hafner, J. Phys. F **5**, 1243 (1975).
[42] J. Hafner, *From Hamiltonians to Phase Diagrams* (Springer, Berlin, 1987).
[43] S. Ichimaru and K. Utsumi, Phys. Rev. B **24**, 7385 (1981).
[44] C. W. Gear, *Numerical Initial Value Problem in Ordinary Differential Equations* (Prentice-Hall, Englewood Cliffs, NJ, 1971), Secs. 9 and 10.
[45] T. Rajasekharan, D. Akhtar, R. Gopalan, and K. Muraleedharan, Nature (London) **322**, 528 (1986).
[46] T. Janssen, Phys. Rep. **168**, 55 (1988).
[47] H. J. Nowak, O. K. Andersen, T. Fujiwara, and O. Jepsen, Phys. Rev. B **44**, 3577 (1991); S. K. Bose, S. S. Jaswal, O.

K. Andersen, and J. Hafner, *ibid.* **37**, 9955 (1988).
[48]W. B. Pearson, *The Crystal Chemistry and Physics of the Metals and Alloys* (Wiley, New York, 1972).
[49]O. Jepsen and O. K. Andersen, Solid State Commun. **9**, 1762 (1971).
[50]J. Hafner, S. S. Jaswal, M. Tegze, A. Pflugi, P. Oelhafen, and H. J. Güntherodt, J. Phys. F **18**, 2583 (1988).
[51]W. Hume Rothery, *The Metallic State* (Oxford University Press, London, 1931).
[52]J. Hafner, in *The Structures of Binary Compounds*, edited by D. G. Pettifor and F. R. de Boer (North-Holland, Amsterdam, 1985), p. 137.
[53]F. Ducastelle and F. Cyrot-Lackmann, J. Phys. Chem. Solids **32**, 285 (1971).
[54]J. E. Graebner and H. S. Chen, Phys. Rev. Lett. **58**, 1945 (1987).
[55]B. D. Biggs, S. J. Poon, and F. S. Pierce, in *Physics and Chemistry of Finite Systems: From Clusters to Crystals*, edited by P. Jena, S. N. Khanna, and B. K. Rao (Kluwer, Dordrecht, 1992), Vol. II, p. 819.
[56]C. M. M. Nex, J. Phys. A **11**, 653 (1978).
[57]M. U. Luchini and C. M. M. Nex, J. Phys. C **20**, 3125 (1987).
[58]U. Mizutani, J. Mater. Sci. Eng. B (to be published).
[59]K. Tanaka (private communication).
[60]N. K. Mukhopadhyay, K. N. Ishihara, S. Ranganathan, and K. Chattopadhyay, Acta Metall. **39**, 1151 (1991).
[61]D. G. Pettifor, J. Chem. Phys. **69**, 2930 (1978).
[62]F. Hippert, L. Kandel, Y. Calvayrac, and B. Dubost, Phys. Rev. Lett. **69**, 2086 (1992).
[63]M. Windisch, M. Krajčí, and J. Hafner, J. Non-Cryst. Solids (to be published).